Hybrid Monte Carlo with Adaptive Temperature in Mixed-Canonical Ensemble: Efficient Conformational Analysis of RNA

ALEXANDER FISCHER, FRANK CORDES, CHRISTOF SCHÜTTE
Konrad–Zuse–Zentrum Berlin, Takustraße 7, D-14195 Berlin, Germany

Received 9 April 1998; accepted 22 June 1998

ABSTRACT: A hybrid Monte Carlo method with adaptive temperature choice is presented that exactly generates the distribution of a mixed-canonical ensemble composed of two canonical ensembles at low and high temperature. The analysis of resulting Markov chains with the reweighting technique shows an efficient sampling of the canonical distribution at low temperature whereas the high temperature component facilitates conformational transitions, which allows shorter simulation times. The algorithm is tested by comparing analytical and numerical results for the small *n*-butane molecule before simulations are performed for a triribonucleotide. Sampling the complex multiminima energy landscape of this small RNA segment, we observe enforced crossing of energy barriers. © 1998 John Wiley & Sons, Inc. J Comput Chem 19: 1689–1697, 1998

Keywords: hybrid Monte Carlo; generalized ensemble; reweighting; *n*-butane; triribonucleotide

Introduction

The efficient sampling of phase space for complex biological systems remains a specific problem in theoretical biochemistry. This problem can only be solved with Monte Carlo (MC) or molecular dynamics (MD) simulations if it is possible to overcome energy barriers, which are large compared to the thermal energy. MC algorithms, which are based on local conformational changes of functional groups, can enforce barrier crossing by significant distortions. Unfortunately, large local distortions are often energetically unfavorable and the corresponding MC proposals will be rejected. One way to overcome this problem is to use hybrid MC (HMC) techniques,[1–3] which allow the combination of global updates in position space with reasonable acceptance rates. Another way is to sample in so-called generalized ensembles[4] where the canonical ensemble is replaced by a probability density, which supports an extended energy range. Higher energy regions will be vis-

Correspondence to: A. Fischer; e-mail: Alexander.Fischer@zib.de

CCC 0192-8651 / 98 / 151689-09

ited more often and produce conformational changes more easily. In this case the resulting Markov chain has to be reweighted according to the canonical ensemble of interest. For the construction of a generalized ensemble, different techniques can be applied.

The classical Ferrenberg–Swendsen scheme[5] uses results from a canonical distribution at one temperature to extrapolate to expectation values of another distribution at a different temperature. But a small difference between the temperatures is necessary to receive statistically reliable results. The reweighting method can be extended to mix data from independent runs.[6] More recently, algorithms were proposed that sample over the whole energy range,[4] like the multicanonical algorithm,[7,8] simulations in a $1/k$ sampling,[9] and simulated tempering.[10] Similar ideas to overcome energy barriers were tested by using Tsallis statistics[11,12] and in the J-walking method.[13] In umbrella sampling[14] generalized ensemble is used to compute the free-energy difference between the system of interest and a reference system.

Another approach is to sample in the canonical ensemble with a modified potential (e.g., fluctuating-potential methods[15]) or other potential smoothing techniques.[16] With these techniques energy barriers can be lowered, but artifacts could be introduced by the deformation of the original potential.

The methods listed above exhibit the following characteristics: first, any of the generalized ensembles has to be adapted to the system of interest either by connecting distribution parameters to the simulation protocol or making a physically motivated initial modification of the energy function. Second, nearly all strategies are based on conventional MC methods. In earlier attempts to perform HMC in generalized ensembles as in ref. 17, peculiarities of the HMC scheme, like the availability of momenta or the possibility of modifications in the acceptance step, are not considered.

In this article we present a specific generalized ensemble that allows us to exploit the advantageous features of HMC. In particular, we propose a mixed-canonical ensemble composed of two canonical ensembles at low and high temperature, which uses the momentum information for introducing an adaptive temperature function and allows a statistical reasonable reweighting to canonical ensemble averages. The resulting method is called adaptive temperature HMC (ATHMC). The only characteristic parameter of the new distribution function can be interpreted in terms of the average potential energy of the canonical ensemble and has to be approximated by an initial simulation. ATHMC still satisfies the detailed balance condition and guarantees statistical convergence. In contrast to umbrella sampling, where comparable generalized ensembles arise, we use the high temperature part to overcome energy barriers rather than as a reference system to compute free energies. However, our main objective is an appropriate adaption of the HMC scheme to such a generalized ensemble.

The general properties of the proposed algorithm can be tested very easily and quickly on small molecules such as *n*-butane. The application to a small RNA segment, the triribonucleotide adenylyl (3′-5′)cytidylyl(3′-5′)cytidin [r(ACC)] should indicate, whether the method can induce conformational transitions in macromolecules with a remarkable number of degrees of freedom. From spectroscopic studies, oligoribonucleotides such as r(ACC) are known to be highly flexible.[18] Fitting experimental data to theoretically generated sampling data of the molecule indicates the coexistence of different conformers at low temperature. The sampling data was generated by MC and MD simulations to reproduce either large-amplitude deformations or rapid internal motions.[18] Therefore, a combination of both approaches within HMC is desirable.

Method

HMC AND GENERALIZED ENSEMBLES

A large class of molecular systems can be described by a separated Hamiltonian of the form

$$H(x, p) = T(p) + V(x) = \tfrac{1}{2} p^T M^{-1} p + V(x). \tag{1}$$

T denotes the kinetic, V the potential energy, and M the diagonal matrix of the atom masses. If an observable A is a function of the coordinates only, the canonical ensemble average is given by

$$\langle A \rangle_\varrho = \frac{\int A(x) \exp[-\beta V(x)]\, dx}{\int \exp[-\beta V(x)]\, dx},$$

where

$$\varrho(x) = \frac{\varrho^*(x)}{Z_\varrho} = \frac{\exp[-\beta V(x)]\,dx}{\int \exp[-\beta V(x)]\,dx}$$

is the corresponding canonical probability density at temperature $\mathcal{T}$ with partition sum Z_ϱ and the so-called inverse temperature $\beta = 1/k_B\mathcal{T}$ (k_B is Boltzmann's constant).

A Metropolis MC method can be used to generate Markov chains of configurations $x^{(k)}$ with $k = 1, \ldots, n$, from which expectation values $\langle A \rangle_\varrho$ of observables A can be calculated by

$$\langle A \rangle_\varrho = \lim_{n\to\infty} \frac{1}{n} \sum_{k=1}^{n} A(x^{(k)}). \qquad (2)$$

Using HMC as a special Metropolis MC algorithm with global updates, the momenta generally serve as the random variable (i.e., new momenta p have to be drawn from a given distribution before each MC step). If we draw the momenta from a Gaussian distribution $\propto \exp[-\beta T(p)]$ according to (1) propose new coordinates x' and new momenta p' by integrating the system through phase space with a reversible and volume preserving discretized flow Ψ^τ (e.g., the Verlet discretization[19]), the new coordinates x' are accepted with a probability of

$$P_{\text{acc}} = \min(1, \exp[-\beta(H(x', p') - H(x, p))]) = \min\left(1, \frac{\varrho^*(x')\exp[-\beta T(p')]}{\varrho^*(x)\exp[-\beta T(p)]}\right).$$

If we want to use the HMC scheme to sample a generalized ensemble $\mu(x) = \mu^*(x)/Z_\mu$, we have to adjust the acceptance probability to

$$P_{\text{acc}} = \min\left(1, \frac{\mu^*(x')\exp[-\beta T(p')]}{\mu^*(x)\exp[-\beta T(p)]}\right) \qquad (3)$$

to satisfy the detailed balance condition. Generally, the inverse temperature β is not given directly by μ, but it has to be chosen appropriately. Thermodynamical averages now have to be calculated by the reweighting method. If the Markov chain generated due to (3) is used to calculate the averages of the quantities $\exp[-\beta V(x)]/\mu^*(x)$ and $A(x)\exp[-\beta V(x)]/\mu^*(x)$, the quotient of these averages results in

$$\lim_{n\to\infty} \frac{\frac{1}{n}\sum_{k=1}^{n} A(x^{(k)}) \frac{\exp[-\beta V(x^{(k)})]}{\mu^*(x^{(k)})}}{\frac{1}{n}\sum_{k=1}^{n} \frac{\exp[-\beta V(x^{(k)})]}{\mu^*(x^{(k)})}} = \frac{\int A(x) \frac{\exp[-\beta V(x)]}{\mu^*(x)} \mu(x)\,dx}{\int \frac{\exp[-\beta V(x)]}{\mu^*(x)} \mu(x)\,dx} = \frac{\int A(x)\exp[-\beta V(x)]\,dx}{\int \exp[-\beta V(x)]\,dx} = \langle A \rangle_\varrho. \qquad (4)$$

Thus, the scalar quantities $\exp[-\beta V(x^{(k)})]/\mu^*(x^{(k)})$ are reweighting factors applied on the configurations $x^{(k)}$ generated from a generalized distribution μ. In contrast to (2), canonical averages of A have to be calculated according to (4). The relative magnitude of the reweighting factors along the Markov chain indicates the statistical reliability of the reweighting scheme, which can be evaluated with histogram techniques.[5]

MIXED-CANONICAL ENSEMBLE

To achieve an improved sampling of coordinate space, we propose a mixed-canonical ensemble with a weighting factor composed as the arithmetic average of two Boltzmann factors at inverse temperatures β^- and β^+:

$$\mu^*(x) = \tfrac{1}{2}(\exp[-\beta^-(V(x) - c)] + \exp[-\beta^+(V(x) - c)]).$$

The principal idea is to enforce barrier crossing by the high temperature part, whereas the low temperature part is important for the statistical reliability of the reweighting. Let $\mathcal{T}$, $\mathcal{T}^-$, and $\mathcal{T}^+$ denote the corresponding temperatures for β, β^-, and β^+. For $\mathcal{T}^- = \mathcal{T}^+$, μ is identical to the canonical ensemble. Moreover, μ converges to the low or high temperature canonical ensemble if c tends to ∞ or $-\infty$, respectively. Although the shift in the potential energy introduced by c has no influence on a canonical ensemble, it determines an energy level in the mixed-canonical density at which weighting according to the low or high temperature changes: if $V(x) - c < 0$, the contribution of β^- will dominate and for $V(x) - c > 0$, the con-

tribution of β^+ will dominate. The persistence in a certain temperature state is controlled by the relation of the parameter c to the potential energy. Because we are interested in expectation values with respect to ϱ, $\mathscr{T}^-$ should be chosen close to $\mathscr{T}$ whereas the $\mathscr{T}^+$ contribution should facilitate energy barrier crossing. Therefore, we can conclude that the sampling prefers the distribution to $\mathscr{T}^-$ if c will be greater than $\langle V \rangle_\varrho$. The difference between c and $\langle V \rangle_\varrho$ determines the amount of sampling at $\mathscr{T}^+$.

HMC WITH ADAPTIVE CHOICE OF TEMPERATURE

For the implementation of the proposed generalized distribution into ATHMC based sampling, we used the following recipe for one update step. Modifications compared to HMC are discussed below. Fixed parameters at the beginning of the procedure are the temperature of interest, the minimal and the maximal temperature of the generalized distribution.

1. Initialization of momenta p at the inverse temperature $\beta(x)$, which is assumed to be known from the previous step,
$$p \propto \exp\left[-\beta(x)\sum_{j=1}^{s}\frac{p_j^2}{2m_j}\right].$$
2. Calculation of new coordinates and momenta $(x', p') = (\Psi^\tau)^n(x, p)$.
3. Computation of $\beta(x')$ due to (6).
4. Acceptance of new coordinates x' with a probability
$$P_{\text{acc}} = \min\left(1, \frac{\mu^*(x')\exp[-\beta(x')T(p')]}{\mu^*(x)\exp[-\beta(x)T(p)]} \times \left(\frac{\beta(x')}{\beta(x)}\right)^{s/2}\right), \quad (5)$$
otherwise stay in old coordinates x; s denotes the number of degrees of freedom.

In contrast to (3), the acceptance probability in (5) is once more generalized, exploiting the special structure of the mixed-canonical ensemble and taking advantage of the fact that detailed balance is satisfied for any arbitrary temperature. Instead of using a constant temperature at each step, we search for a temperature function $\beta = \beta(x)$, which depends on the actual potential energy in such a way that the Boltzmann factor at $\beta(x)$ is equal to $\mu^*(x)$. This results in the temperature function (Fig. 1)

$$\beta(x) = -\frac{\ln \mu^*(x)}{V(x) - c}. \quad (6)$$

(For states x with $V(x) = c$, the temperature $\beta(x)$ has to be evaluated by interpolation.)

With this choice of temperature we can sample from μ in a way that reflects the ''local'' behavior of the density: starting a trajectory at x with momenta drawn from a Gaussian distribution corresponding to $\beta(x)$ and arriving at a configuration x' with $\Delta\beta = \beta(x') - \beta(x) \approx 0$, results in an acceptance rate as is typically achieved in HMC. Especially the sampling in low energy regions is dominated by the Boltzmann factor corresponding to β^- with $\beta(x) \approx \beta^-$ and vice versa in high energy regions with $\beta(x) \approx \beta^+$. In these cases $\Delta\beta$ is low, even if larger changes in the potential energy occur. For other values of $\Delta\beta$ the potential and momenta part of the acceptance step (5) fit together and result also in a reasonable acceptance rate. Therefore, we can expect an acceptance rate close to the corresponding one in an HMC scheme.

Another modification of the acceptance probability (5) comes along with the adaptive temperature. The additional factor $(\beta(x')/\beta(x))^{s/2}$ in (5) results from the normalization of the two different

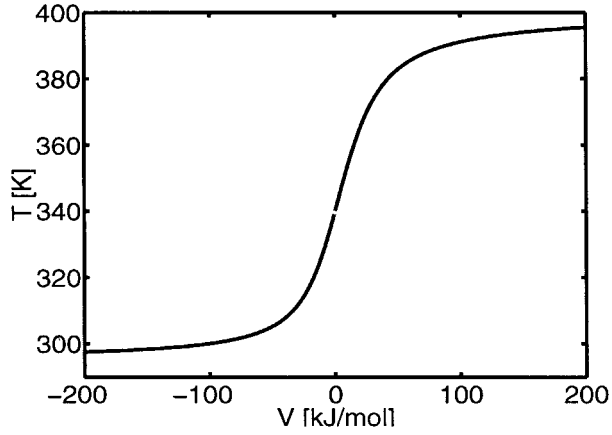

FIGURE 1. Choice of temperature $\mathscr{T}(x)$ in dependence of the potential energy with $\mathscr{T}^-$ = 295 K, $\mathscr{T}^+$ = 400 K, and $c = 0$. Note that the temperature function is directly connected to μ^* and reflects the density of the mixed-canonical ensemble. A change of c induces a change in the density of μ and a shift of the temperature function.

momentum distributions for $\beta(x)$ and $\beta(x')$, which differ in their standard deviation. Because β remains fixed in HMC, this factor simplifies to 1 [see, e.g., eq. (3)]. Indeed, with this factor detailed balance is satisfied for ATHMC: the probability to be in x and to draw the momenta p is given by $\mu(x)\exp[-\beta(x)T(p)]\,dx\,dp$. Furthermore, the discrete flow Ψ will propose deterministically the configuration $(\Psi^\tau)^m(x, p) = (x', p')$, where τ and m are fixed parameters determining the HMC stepsize τm.

Due to the reversibility of Ψ, applying the Metropolis criterion to guarantee detailed balance[3] results in

$$P_{\mathrm{acc}}((x, p) \to (x', p')) = \min\left(1, \frac{\mu(x')\dfrac{\exp[-\beta(x')T(-p')]}{\int \exp[-\beta(x')T(-p')]\,d(-p)}}{\mu(x)\dfrac{\exp[-\beta(x)T(p)]}{\int \exp[-\beta(x)T(p)]\,dp}} \frac{dx'\,d(-p')}{dx\,dp}\right).$$

We have $dx'\,d(-p')/dx\,dp = 1$, because ψ is volume preserving so that a simplification of the normalization constants of the momenta yields (5).

The temperature function and the mixed canonical ensemble are simultaneously influenced by the parameter c. Let us assume that c is somewhat larger than the average potential energy with respect to ϱ. Then the density of the generalized ensemble will enclose the canonical one but also cover higher energy regions, which has no significance in ϱ. In our case this mean that whenever the potential energy increases in the vicinity of c, kinetic energy is pumped into the system according to the choice of higher temperature for the generation of momenta. Additionally, proposals with higher energy are accepted more easily in μ and the system can move toward higher energy regions where conformational changes happen more often. Conversely, the system can move from high to low energy regions and eventually arrive in another conformation. Therefore, the fluctuations of $\beta(x)$ serve as a good indicator for the desired behavior and can be used in preliminary runs to find a suitable value for c.

MODEL SYSTEMS

The proposed method was tested on two model systems. The *n*-butane molecule is a very small organic compound. The linear chain consists of four carbons and 10 hydrogens. The configuration of the heavy atoms can be described by one torsion angle, two bond angles, and three bonds. Significant conformational changes are especially effected by torsion angle rotations. The semiempirical Hamiltonian, which is conventionally used to mimic covalent and noncovalent energy contributions of this kind of macromolecules, consists of terms for the kinetic energy, and in its simplest form for bond- and angle oscillations and torsion angle rotations:

$$\begin{aligned} H(\mathbf{q}, \mathbf{p}) = {} & \tfrac{1}{2}\mathbf{p}^T M^{-1}\mathbf{p} \\ & + \sum_{\text{bonds}} V_{\text{bonds}} + \sum_{\text{angles}} V_{\text{angles}} \\ & + \sum_{\text{torsions}} V_{\text{torsions}} \\ & + \sum_{\text{atom pairs}} (V_{\text{Lennard-Jones}} + V_{\text{Coulomb}}) \end{aligned}$$

For *n*-butane we used the extended atom model of Ryckaert and Bellemans[20] (Fig. 2), which reduces the representation of the chain to the carbon atoms. Moreover, the so-called nonbonded Lennard–Jones and Coulomb interactions play no role for *n*-butane, because interactions up to the third neighbors are totally covered by the covalent terms. The *n*-butane molecule with its one torsion angle ω serves as an ideal test system for the proposed ATHMC scheme. First, the three orientations of ω also describe the three possible conformations (see

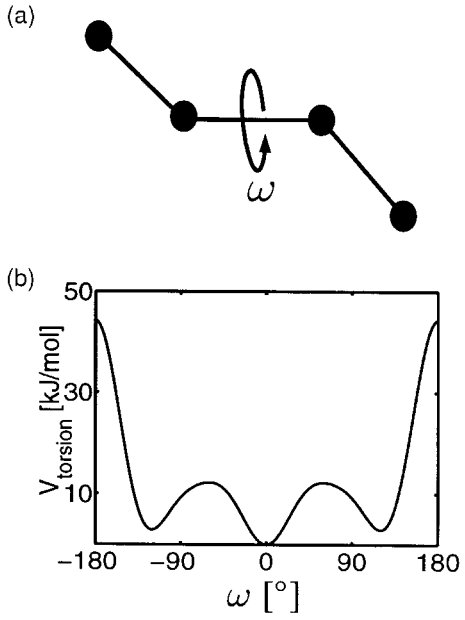

FIGURE 2. (a) Extended atom model of *n*-butane with the torsion angle ω. (b) Torsion angle potential. The main minimum corresponds to the trans orientation of the angle, the two side minima to the $\pm$gauche orientations.

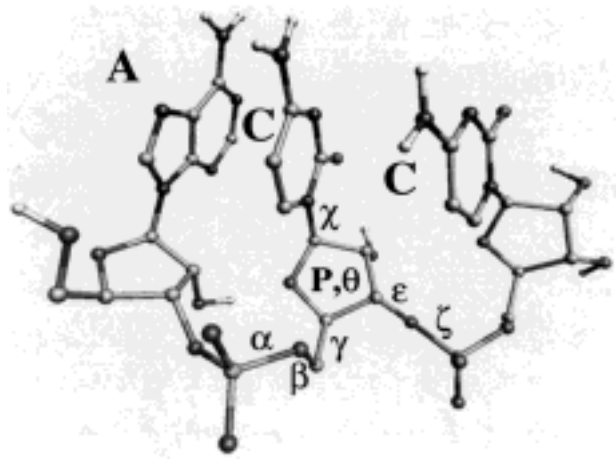

FIGURE 3. The triribonucleotide adenylyl(3′-5′)cytidylyl(3′-5′)cytidin [r(ACC)] in the extended atom representation of GROMOS96.[22] A and C denote the bases adenine and cytosine. Small greek letters refer to the set of torsion angles, which is necessary for a rough reconstruction of the molecule's configuration. The torsion angles of the ribose can be approximated by the pseudorotation angle P and the phase θ.[23]

Fig. 2). Second, as was shown in ref. 21, the expectation value for the torsion angle potential V_{torsion} can be computed analytically. Therefore, we can compare our results with analytically exact values.

The physical representation of the triribonucleotide (Fig. 3) r(ACC) is based on the GROMOS96 extended atom force field.[22] Comparable to the *n*-alkane model, some nonpolar hydrogens are covered by the corresponding heavy atoms. Moreover, GROMOS96 contains an extra covalent energy term for out of plane oscillations. The global structure of r(ACC) can be roughly described by eight parameters per nucleotide (Fig. 3). The torsion angles χ around the glycosyl bond and the puckering of the ribose ring described by the pseudorotation angle P and its phase θ (ref. 23) are of special interest for the conformational analysis.

Results and Discussion

n-BUTANE MOLECULE

For simulations of *n*-butane, we used the Verlet scheme[19] with $n = 40$ iterations and a time step of $\tau = 15$ fs, which results in a trajectory length of 600 fs for each update step. Performing a simulation over 10^5 steps at a temperature of $\mathcal{T} = 100$ K with HMC (not shown here), we observed a trapping of the Markov chain in the $+$gauche conformation, which is where we started the simulation. The energy barrier toward the trans conformation seems to be too high at this low temperature to be overcome in a reasonable simulation time.

Sampling the position space with ATHMC with only 10^4 steps (Fig. 4) and carrying out the reweighting (4) to the temperature of interest at $\mathcal{T} = 100$ K leads us to a distribution of the three conformations of ω and to an expectation value of $\langle V_{\text{torsion}} \rangle$ close to the analytic values:

	$\langle V_{\text{torsion}} \rangle$	−Gauche (%)	Trans (%)	+Gauche (%)
Analytic values	0.571	2.40	95.20	2.40
HMC	3.353	0	0	100
ATHMC (reweighted)	0.580	3.15	94.24	2.61

The simulations on *n*-butane in μ were easily adapted to a suitable parameter set by short preliminary runs without the need of fine-tuning. The acceptance rate decreased only slightly from 83.1 to 75.3% by changing from HMC to the ATHMC scheme.

Figure 4 illustrates that a change of the torsion angle orientation is directly correlated to the choice of temperature. We can observe the behavior as

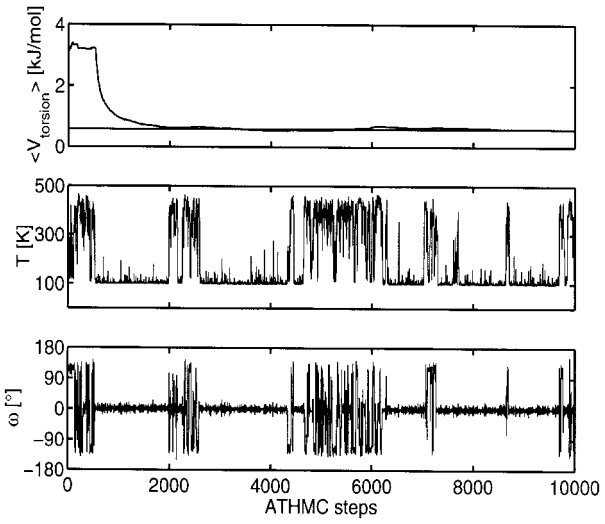

FIGURE 4. ATHMC run for *n*-butane. The simulation was performed for 10^4 steps with $\mathcal{T} = 100$ K, $\mathcal{T}^- = 90$ K, $\mathcal{T}^+ = 500$ K, and $c = 1.5$. The flat line in the first subplot indicates the analytically computed expectation value.

described in the previous section. Note that most of the time the Markov chain samples at $\mathcal{T} \approx \mathcal{T}^-$, which guarantees the statistical reliability of the reweighting.

TRIRIBONUCLEOTIDE r(ACC)

HMC simulations on r(ACC) were performed over $5 * 10^5$ steps. The discretized flow was again realized by the Verlet integrator[19] with a time step of $\tau = 2$ fs over $n = 40$ iterations between two HMC updates. Compared to *n*-butane, a much smaller time step and MD-trajectory is required to guarantee an acceptance rate of 58.7%. The c parameter for the ATHMC calculations was first adjusted to an approximated averaged potential energy, which results from preliminary short HMC cycles. In subsequent short test calculations c was then slowly shifted toward higher energies. The preprocessing was finished at a total shift of 50 kJ/mol. At this point a temperature fluctuation between $\mathcal{T}^- = 295$ K and $\mathcal{T}^+ = 400$ K was reached, which basically prefers the low temperature (Fig. 5). The adjustment of c strongly depends on the difference between the two temperatures and the expected energy fluctuations of the simulation. The butane molecule with only a few degrees of freedom allows larger jumps in temperature or kinetic energy. It appears that the ATHMC finds pathways from low to high energy regions. Test calculations for the triribonucleotide on the other hand

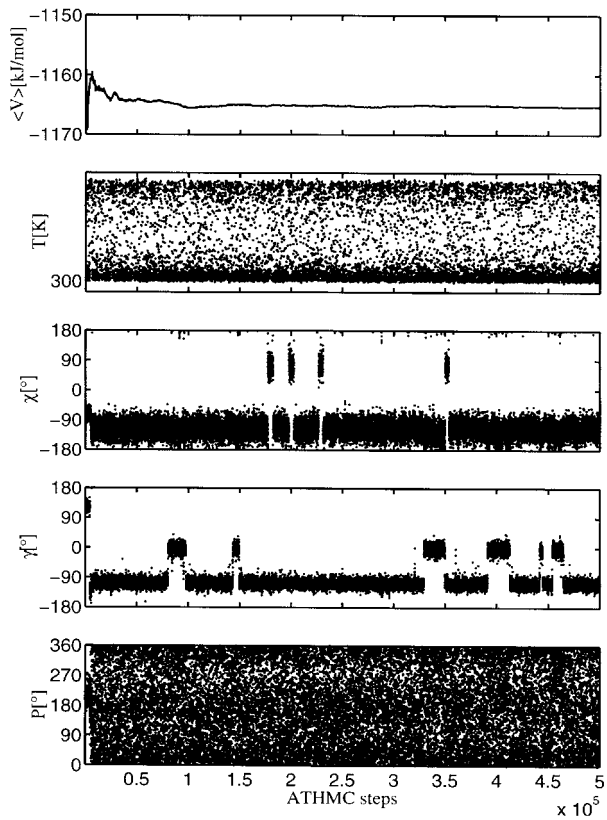

FIGURE 5. ATHMC run for r(ACC). The simulation was performed for $\mathcal{T}^- = 295$ K, $\mathcal{T}^+ = 400$ K, and $c = -1121$ kJ / mol. The averaged potential energy $\langle V \rangle$, the temperature $\mathcal{T}$, and for the cytidylyl group the torsion angles χ and γ and the pseudorotation angle P are displayed at every 20th step.

show that at $\mathcal{T}^+ = 500$ K, r(ACC) could be brought into a high energy state during the simulation, but it will not relax again. Large temperature differences will narrow the range around c in which a moderate transition between the two corresponding energy regions can take place.

The development of the averaged potential energy in ATHMC (Fig. 5) and HMC (Fig. 6) demonstrates the superiority of the adaptive temperature choice in the mixed-canonical ensemble. The averaged energy converges faster to a slightly lower value. Although the temperature difference of 105 K is smaller than in the *n*-butane case and the global updates are based on shorter MD simulations, Figure 6 illustrates the ability of the method to induce global conformational changes. This behavior should be examined on some selected parameters of the cytidylyl group. The torsion angle around the glycosyl bond χ mainly oscillates in the range between $-160°$ and $-80°$ but is shifted

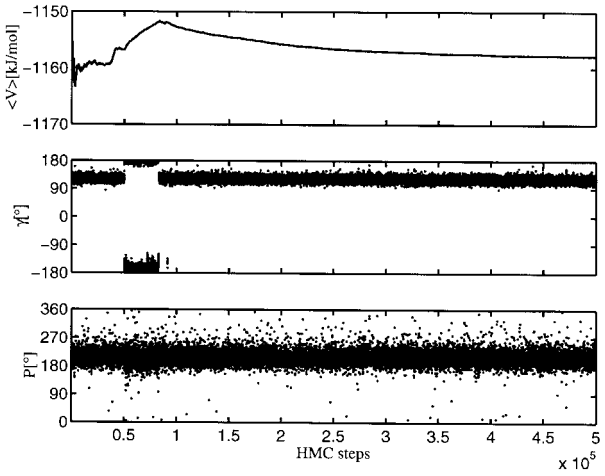

FIGURE 6. HMC for r(ACC) in the canonical ensemble. The simulation was performed for $\mathscr{T} = 300$ K. The averaged potential energy $\langle V \rangle$ and for the cytidylyl group the torsion angle γ and the pseudorotation angle P are displayed at every 20th step.

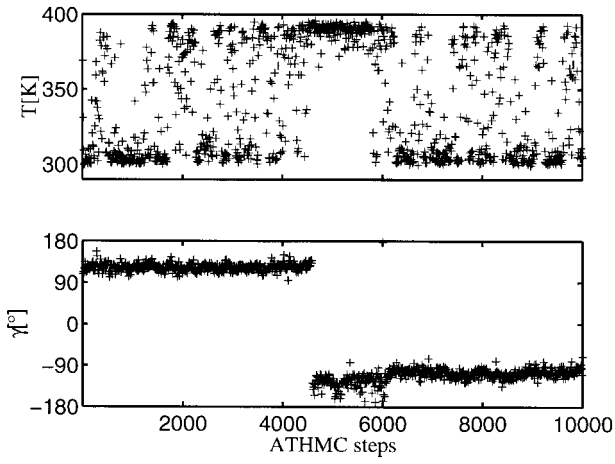

FIGURE 7. ATHMC for r(ACC) in the mixed-canonical ensemble. The simulation was performed for $\mathscr{T}^- = 295$ K, $\mathscr{T}^+ = 400$ K, and $c = -1121$ kJ / mol. The temperature $\mathscr{T}$ and for the cytidylyl group the torsion angle γ are displayed at every 10th step over the first 10,000 steps.

at least 4 times toward the range between 40° and 100°. Even more conformational transitions can be observed in the backbone for the torsion angle γ.

The backbone transitions are clearly uncoupled from the glycosyl transitions but are highly correlated to the dynamics of the other internal coordinates of the backbone, β, ϵ, and ζ (not shown here). In our simulations the torsion angle α shows no distinguishable transitions, whereas the pseudorotation angle P is spread over its whole definition range.

These results of ATHMC are in contrast to normal HMC, which should be discussed for γ and P (Fig. 6). In HMC γ remains almost in the initial state. The only exception at the beginning between 50,000 and 80,000 steps probably results from the equilibration of the system, which is not finished at this stage. Additionally, the ribose ring described by the pseudorotation angle P and the phase θ clearly occupies only one preferred conformation. The averaged potential energy converges very slow and stays slightly above the value of ATHMC. Again HMC is not able to enforce the necessary conformational changes, which bring the system into more preferable conformations. Moreover, Figures 5 and 6 demonstrates that ribose puckering is very sensitive to the temperature.

To investigate the dependence between the temperature choice and conformational transitions in more detail, we now zoom to the first 10,000 steps of the ATHMC run (Fig. 7). The averaged potential energy in Figures 5 and 6 indicates that the arbitrarily chosen initial conformation of the simulation belongs to an energy below the average, which makes a transition to another more realistic conformation desirable. The γ torsion at this starting point is around 120°. Normal HMC (Fig. 6) is unable to induce a necessary transition to another state. Only the heating of the system due to the choice of momenta according to higher temperature induces the necessary transition of γ around step 4500.

The fact that ATHMC samples at different temperatures with sufficient rates is furthermore illustrated by the probability distribution of energy before and after the reweighting (Fig. 8). Without reweighting [eq. (4)] we observe a maximum around the averaged potential energy, but another distribution peak for higher energies is exactly enforced by the choice of higher temperatures and the nonnegligible acceptance at higher energies. Figure 8 makes the strategy of generalized ensembles very clear: to overcome energy barriers by sampling in not only low but also high energy areas. The idea of equalizing the energy distribution over an extended energy range finds its extreme realization in the multicanonical approach,[4] which is orientated on a constant distribution. ATHMC also stretches the energy distribution but is conceptionally still connected to the physical properties of the system, which is indicated by the

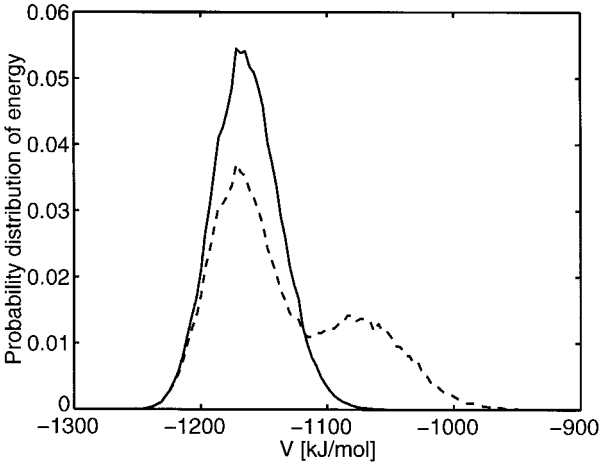

FIGURE 8. ATHMC for r(ACC) in the mixed-canonical ensemble. Probability distribution of energy (- - -) before and (——) after reweighting. Computed according to eq. (4).

great overlap of canonical and mixed-canonical distribution.

Conclusion

The ATHMC method presented herein permits the realization of an adaptive temperature choice in a generalized ensemble. The crucial detailed balance condition remains to be valid in ATHMC, because the separation of coordinates and momenta in the acceptance step is possible.

The comparison of conventional HMC and ATHMC exhibits the superiority of the latter with respect to the conformational analysis of biomolecules. The adaptive temperature choice coupled with a generalized, mixed-canonical ensemble was shown to be responsible for the efficient sampling properties. Like all other strategies based on generalized ensembles, the proposed algorithm cannot relinquish pre- and postprocessing procedures. But preprocessing in ATHMC needs only one parameter, c, which corresponds to the averaged potential energy of the system. The simplicity of this approach may be advantageous for applications to larger molecules, because even an insufficient determination of c will give reliable statistical results: if c deviates too much from its optimal value, one of the canonical distributions will dominate the sampling. Moreover, the influence of c on the temperature fluctuations can even control the equilibration state of the system.

In a forthcoming work it will be of special interest to include the solvent environment into ATHMC in order to investigate its influence on temperature choice, determination of c, and acceptance rate. The inclusion of a solvent is the necessary precondition for quantitative comparison with other theoretical, as well as experimental, data on oligoribonucleotides.

References

1. S. Duane, A. Kennedy, B. Pendleton, and D. Roweth, *Phys. Lett. B*, **195**, 216 (1987).
2. A. Brass, B. Pendleton, Y. Chen, and B. Robson, *Biopolymers*, **33**, 1307 (1993).
3. B. Mehlig, D. Heermann, and B. Forrest, *Phys. Rev. B*, **45**, 679 (1992).
4. U. Hansmann and Y. Okamoto, *J. Comput. Chem.*, **18**, 920 (1997).
5. A. Ferrenberg and R. Swendsen, *Phys. Rev. Lett.*, **61**, 2635 (1988).
6. A. Ferrenberg and R. Swendsen, *Phys. Rev. Lett.*, **63**, 1195 (1989).
7. B. Berg and T. Neuhaus, *Phys. Lett. B*, **267**, 249 (1991).
8. U. Hansmann and Y. Okamoto, *J. Comput. Chem.*, **14**, 1333 (1993).
9. B. Hesselbo and R. Stinchcombe, *Phys. Rev. Lett.*, **74**, 2151 (1995).
10. E. Marinari and G. Parisi, *Europhys. Lett.*, **19**, 451 (1992).
11. I. Andricioaei and J. Straub, *Phys. Rev. E*, **53**, 3055 (1996).
12. I. Andricioaei and J. Straub, *J. Chem. Phys.*, **107**, 9117 (1997).
13. D. Frantz, D. Freeman, and J. Doll, *J. Chem. Phys.*, **93**, 2769 (1990).
14. G. Torrie and J. Valleau, *J. Comput. Phys.*, **23**, 187 (1977).
15. Z. Liu and B. Berne, *J. Chem. Phys.*, **99**, 6071 (1993).
16. B. Berne and J. Straub, *Curr. Opinion Struct. Biol.*, **7**, 181 (1997).
17. U. Hansmann, Y. Okamoto, and F. Eisenmenger, *Chem. Phys. Lett.*, **259**, 321 (1996).
18. N. Bouchemal−Chibani, C. du Penhoat, M. Abdelkafi, M. Ghomi, and P. Turpin, *Biopolymers*, **39**, 549 (1996).
19. L. Verlet, *Phys. Rev.*, **159**, 98 (1967).
20. J.-P. Ryckaert and A. Bellemans, *Faraday Discuss.*, **66**, 95 (1978).
21. A. Fischer, Diploma thesis, Freie Universität, Berlin, 1997.
22. W. van Gunsteren, S. Billeter, A. Eising, P. Hünenberger, P. Krüger, A. Mark, W. Scott, and I. Tironi, *Biomolecular Simulation: The GROMOS96 Manual and User Guide*, vdf Hochschulverlag AG an der ETH Zürich, Zürich, 1996.
23. C. Altona and M. Sundaralingam, *J. Am. Chem. Soc.*, **94**, 8205 (1972).